

Early adaptive resistance to Afatinib in PC9 cells

Rick Mulders - 3779173

[Layman's summary](#)

Targeted therapies are commonly used to treat cancer. These therapeutics are made to target and break specific parts of the molecular machinery that causes cancer cells to grow uncontrollably. The smoking-related non-small-cell lung cancer (NSCLC) relies, in 60% of cases, heavily on Epidermal Growth Factor (EGF). EGF signals for cells to grow and this cancer type produces many more EGF receptors (EGFR) than it should, receiving many more growth signals than it should. Drugs that block EGFR signaling, like gefitinib and erlotinib proved to be an effective targeted therapy. However, prolonged treatment resulted in drug-resistant cancer cells, due to mutations in EGFR. New drugs were developed against this EGFR mutant, like afatinib, but once again the cancer would come back having acquired a resistance to the first and second line of drugs. It was discovered that upon the initial treatment with these cancer drugs, a fraction of the cells would survive and that from these cells a resistant cancer would grow. Even if the mutations that cause drug resistance are not present in any cancer cells at the time of treatment, a portion would still survive. In this study, we took a look at the proteins that make up the molecular machinery of NSCLC cells. We observed how adaptations in the regulation of this machinery allowed these cancer cells to survive. We discovered that only cells which are closest to each other survive afatinib treatment and that they make stronger connections between each other. Through these connections, they signal to each other to survive and after three days, to grow again. Inhibiting these survival signals at the same time as afatinib treatment may be enough to prevent cancer recurrence.

[Abstract](#)

Non-Small-Cell Lung Cancer (NSCLC) is a prevalent cancer type in smokers. 60% of NSCLCs have overexpression of Epidermal Growth Factor Receptor (EGFR). Tyrosine Kinase Inhibitors (TKI) are drugs that target Tyrosine Kinase Receptors (RTK) like EGFR and inhibit their function. EGFR specific TKIs, like gefitinib, are used to treat NSCLC. Prolonged gefitinib treatment can result in cancer recurrence with an acquired resistance to gefitinib, like EGFR-T790M. Afatinib is a TKI that works specifically on EGFR-T90M, but just like with gefitinib cancer can return with an acquired afatinib resistance. In this study, we explored the mechanics of adaptive resistance in homogenous NSCLC cell line PC9 of which a portion survives initial afatinib treatment and was able to regain cell growth in this condition. We observed a morphological response in islet clustering and reduced motility, suggesting cell density as a resistance

factor. Using proteomics and phosphoproteomics we were able to trace protein expression and regulatory adaptations as PC9 cells became afatinib resistant. We saw an increase in EGFR expression within a day, restoring activity, however, activity was lost over time. Before additional EGFR could be expressed and after activity loss, there was upregulation of MET, Erbin, and Cav1. This suggested compensatory roles for these or associated proteins, like TIE2. Inhibitive phosphorylation of JAK2 by JAK2JH2 was reduced, likely mitigating the effect of EGFR inhibition. Additionally, there was constitutive upregulation of NCK1 and paxillin which facilitate cross-talk of RTKs like MET and EGFR with Integrins. Clustered morphology, upregulation of Integrin based signaling, and possible TIE2 upregulation suggest a central role for cell-cell interactions for adaptive resistance to TKI in NSCLC.

Introduction

Background

Cancer is an umbrella term for a set of diseases that share a common trait, uncontrolled cell growth. At the basis of any cancer lies a series of genetic mutations, which cumulatively predispose the cells in which they occur, to develop tumours¹⁻³. The genes which, when mutated, can contribute to malignant growth are classed into two categories, proto-oncogenes, and tumour-suppressor genes. Proto-oncogenes become oncogenes when a mutation occurs which promotes cell growth, directly or indirectly. This is not limited to nucleotide alterations within a gene but also copy number increases, such is often the case with Epidermal Growth Factor Receptor (EGFR, ERBB1)^{4,5}. EGFR transduces signals for a cell to grow, so increasing the number of copies of this gene leads to additional growth signals, making it an oncogene. Tumour-suppressor genes code for proteins with protective functions, correcting errors or forming stop gaps for important processes. As an example, P53 is an essential protein for engaging programmed cell death (apoptosis) as a last resort for cells damaged beyond repair⁶. P53 is a tumour-suppressor gene that is often rendered inactive through mutation in a wide variety of cancer types, allowing carcinogenesis to continue unabated. Furthermore, cancer differs in genetic profile depending on the person or tissue of origin. Even within cell types, different cancer types may occur¹. Mesenchymal tumours differ genetically from epithelial tumours, lung cancers differ genetically from breast, skin, or intestinal cancers, and lung cancer in smokers is often genetically distinct from those in non-smokers. In the meantime, some cancer types across cell types may display similar genetic mutations not shared by cancer types of the same original cell type. As such, cancers are better characterized by their molecular particularities than a phenotypic propensity to grow uncontrollably.

Non-Small-Cell Lung Cancer (NSCLC) is a lung cancer type commonly found among smokers. In over 60% of NSCLC cases, EGFR is overexpressed, usually through gene copy increases or through preventing EGFR degradation^{5,7}. EGFR overexpression indicates that NSCLC is particularly reliant on EGFR signaling and can be exploited in the treatment of NSCLC. The principle of exploiting a specific oncogenic molecular modus operandi to treat cancer is called targeted therapy.

Targeted therapies were first used to successfully treat cancer in 1988⁸. Early targeted therapeutics concern monoclonal antibodies which can reversibly block ligand-receptor interactions and thereby disrupt signal transduction pathways on which the cancer relied. Small molecules or drugs were added to an expanding arsenal of molecules used for targeted therapies^{9,10}. Drugs can bind irreversibly and pass through cell membranes, expanding the scope of possible targets. This allows for a selection of specific therapeutics on the basis of a genetic profile. Additionally, due to intervention on specific aberrant molecular signaling, the damage to healthy cells is mitigated. This reduction in collateral damage to healthy tissue makes targeted therapies an attractive alternative to surgery, chemotherapy, or radiotherapy^{11,12}. For the treatment of the aforementioned EGFR dependent NSCLC a class of targeted therapeutics also exists^{5,12}. Tyrosine kinase inhibitors (TKI) are monoclonal antibodies or drugs which block the signaling capability of tyrosine kinase receptors (RTK) such as EGFR by occupying the ligand binding spot or by blocking dimerization and cross-kinase activation intracellularly (Fig. 1A). One of the first EGFR targeting TKI drugs is gefitinib, which successfully causes NCLS remission. However, prolonged gefitinib use eventually results in recurrence with an acquired resistance to gefitinib. This resistance is caused by a number of mutations on the EGFR gene itself, most commonly by a substitution of Threonine with methionine at position 790 on the protein (T790M)^{7,13,14}. This leads to the development of a second line of EGFR targeting TKIs. Afatinib is one such TKI that specifically targets T790M mutant EGFR. Patients which acquire a resistance to gefitinib can continue to be treated with afatinib instead¹⁵⁻¹⁷. Acquired drug resistance is a phenomenon that is observed in other cases of targeted therapy as well and it leads to a question^{18,19}. How does a fraction of cells survive the initial exposure to a targeted therapeutic?

There are two hypotheses that could explain targeted therapy survival. The first posits that the tumour is heterogenetic. There is a pre-existing subpopulation that has a drug-resistant allele which is selected for by the drug^{20,21}. The second hypothesis forgoes the necessity for heterogeneity within the initial population, instead suggesting a form of resistance akin to antibiotic resistance in bacteria. If a fraction of the initial homogenetic cell population can survive treatment, pressure induced by the drug may force an adaptive restructuring of signaling pathways. This allows cells to grow in the presence of the drug and

acquire genetic resistances within such an environment²². To analyse adaptive responses on an intracellular level without prior knowledge of mechanisms underlying adaptive resistance requires a holistic approach. Including the whole of a cellular phenomenon is referred to as “omics”, such as genomics, transcriptomics, metabolomics, methylomics, or proteomics²³. These omics correspond with different stages of the central dogma in biology and should be selected based on relevancy. The adaptive resistance hypothesis proposes a response at the level of signaling pathways that are governed by proteins and would fit a proteomic analysis²⁴.

Proteomics and Mass Spectrometry

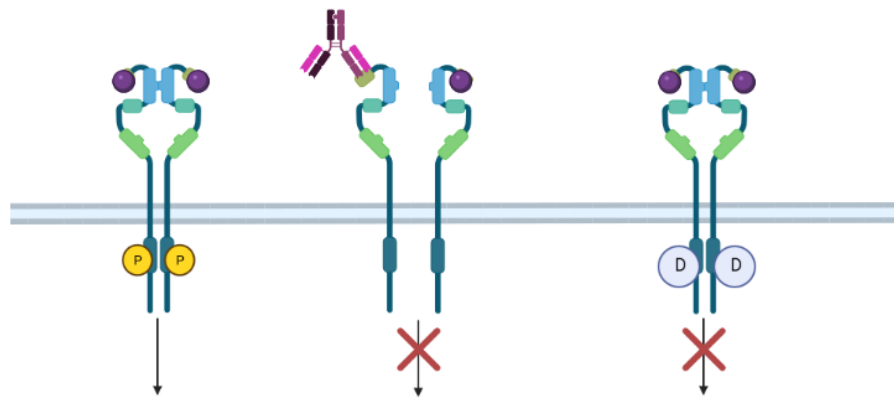
Proteomics is the study of proteomes and a proteome is the total sum of proteins present in a sample at a certain time-point. Phosphoproteomics is the study of phosphorylated proteins within a proteome through enrichment of phosphorylated proteins prior to analysis. Proteomic analysis is done on a mass spectrometer (MS), which allows the identification of molecular particles based on their measured mass/charge ratio. While proteins can be intact, proteolytic digestion increases the efficiency of liquid chromatography and allows for further fragmentation within the mass spectrometer, both allow for a higher resolution MS analysis. The combination of Liquid chromatography and Mass spectroscopy is a form of two-dimensional chromatography, this allows for less noisy measurements by the separation of analytes which could produce interfering signals in one-dimensional chromatography. Trypsin cleaves polypeptide chains after an arginine or lysine which results in peptides that can be traced back to specific proteins. The mass-spectrometer used here is a Q-exactive, an orbitrap quadrupole mass spectrometer connected to a Liquid Chromatography system (LC-MS/MS)^{25,26}(fig. 1B). High pH liquid chromatography separates peptides according to hydrophobicity prior to entering MS. Eluting peptides are ionized through electrospray ionisation (ESI), forming charged aerosols which provides them with a charge-over-mass ratio (m/z). Peptides are ionized at the carboxyl and amino ends of the peptide chain as well as any susceptible functional groups which mean they have a charge of at least 2. The ions then pass from atmospheric pressure into a vacuum with the help of an S-lens, this is a compartmentalised funnel where each compartment lowers the pressure. Electromagnetic quadrupoles then select for ions in a range of m/z to pass on to the analyser, this range can be adjusted as is required. The C-trap allows ions to pass through to the orbitrap analyser directly or the Higher-energy C-trap dissociation (HCD) where ions get fractionated further and then the orbitrap analyser. The orbitrap analyser is an electromagnet that traps ions to orbit the electrode, these ions oscillate along the longitudinal axis of the spindle in a way particular to their m/z value. In tandem MS (MS/MS) ionised peptides are first measured whole (MS1), then selected on m/z for fractionation and analysed again (MS2). Using Fourier transformation, the oscillations of specific ions can

be isolated and identified. This results in a graph of peaks that correspond to known peptides and can thus be identified using database searching. While mass-spectrometry does measure abundance, this is not an absolute value and can therefore not be used for absolute quantification. In order to generate reliable relatively Quantified proteomic data, an internal standard needs to be used. This can be achieved through stable isotope labelling by amino acid in cell culture (SILAC) in which a parallel cell culture is grown in medium containing essential amino acids containing a number of stable carbon-13 isotopes and thereby made “heavy” as opposed to the unaltered “light” sample²⁷(fig. 1C). In the case of this study, a negative control was labelled heavy with Arginine-6 (6 ¹³C isotopes) and lysine-4 (4 ¹³C isotopes) then used as an internal standard by mixing equal parts heavy to each light sample. Because the measured abundance of heavy peptides is constant between samples, the relative abundance of light peptides between samples can be determined.

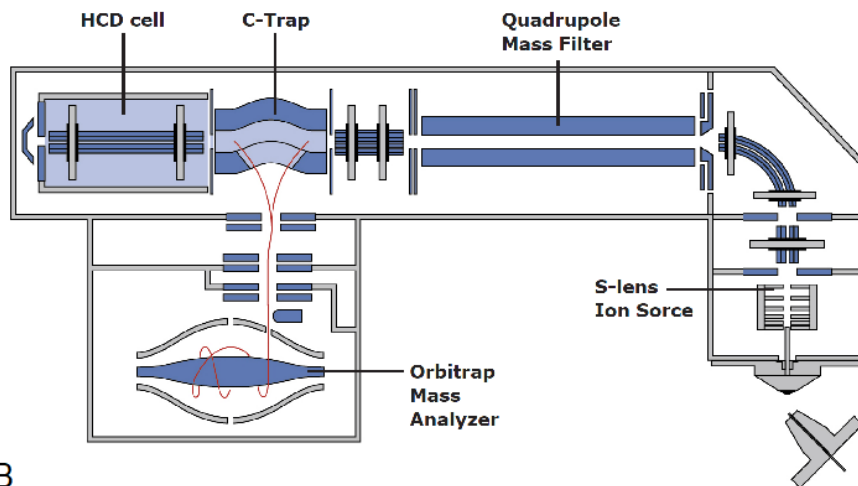
Phosphorylation and signaling

The proteomic data tells us about the regulation of protein networks at the level of protein expression. However, Proteins are subject to post-translational regulation, these could be required to activate or inhibit protein function and do so irrespective of protein expression levels. The major regulatory processes are phosphorylation and ubiquitination. The latter is mostly involved in marking proteins for lysosomal destruction and the former plays a key role in many signal transduction pathways. Kinases are the catalysts that facilitate phosphorylation of specific serine/threonine or tyrosine residues of specific proteins. The specificity of residue phosphorylation tightly controls signaling pathways. The phosphorylation status of these residues or phosphosites can be assessed using phosphoproteomics to indicate protein activity in conjunction with proteomics. It is important to note that post-translational modification is always in a background of expression, therefore changes in expression are reflected in phosphoproteomics and need to be taken into account. Phosphoproteomics follows the same steps as proteomics with one additional step prior to MS, Phosphopeptide enrichment. In this study, we were interested in the effects of Tyrosine Kinase inhibition and as such, we used phosphotyrosine immunoprecipitation (pY-IP)²⁸. Agarose beads containing Phosphotyrosine antibodies on the surface bind any peptides with phosphorylated tyrosine in a digested cell lysate. These form a pellet when centrifuged containing only phosphotyrosine peptides for phosphoproteomic analysis.

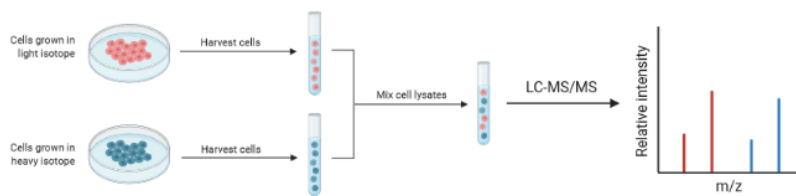
In summary, using proteomics and phosphoproteomics we explored adaptations, on a protein expression and phosphorylation level, that allow a subset of homogenetic EGFR dependent NSCLC cells to survive afatinib treatment.



A



B



C

Figure 1: Diagrams adapted from Biorender.com (A, C) and wur.nl (B). **A** Left to right: EGFR activation, Monoclonal antibody based inhibition of EGFR, Drug based inhibition of EGFR. **B** Q-exactivePlus Orbitrap mass spectrometer for LC-MS/MS **S-lens** Introduces ions to vacuum. **Quadrupole mass filter** Captures ions within an m/z range to pass on. **C-trap** holds ions coming from quadrupoles and fragmented ions from HCD cell. **HCD cell** Fragments ions through collision with a gas. **Orbitrap mass analyser** measures m/z of ion fragments based on oscillations over the length of the analyser. **C** A schematic overview of stable isotope labelling by amino acid in cell culture (SILAC).

Results

Cell line selection and properties

To assess the process by which resistance develops in EGFR dependent cancer types we first required a suitable model. To this end, we tested several NSCLC cell lines for afatinib responsiveness using almar blue cell viability assay 72 hours after treatment with increasing afatinib dosage from 0.1 to 1,000 nanomole per litre (nM) PC9 appeared most responsive to low doses of afatinib and more resilient to high doses of afatinib than other cell lines, for example, H1975 (fig. 2A). At 1 nM and 100 nM afatinib EGFR Y1068 phosphorylation is inhibited more effectively in PC9 cells than in H1975 cells (fig 2B). At high doses of afatinib cytotoxicity occurs. The effective dose for the rest of the study was set at 10 nM Afatinib, which is enough to induce a full response in PC9 cells. PC9 cells were treated with 10 nM afatinib 24 hours after plating through medium replacement, and observed during continual exposure. 24 hours after treatment initiation, morphological differences between treated and untreated cells became apparent(fig. 2C). Treated cells were smaller and concentrated in islets, leaving large open areas. This is in contrast to untreated PC9 cells which spread out over the surface evenly. Cell growth was tracked for 144 hours using the Incucyte system (fig. 2D). At the 24 hour mark cells were treated with 10 nM afatinib. Cell growth was inhibited until the 72 hour mark. From this point cell growth was reinitiated and reached full confluency at 144 hours, 120 hours after introduction of 10 nM afatinib.

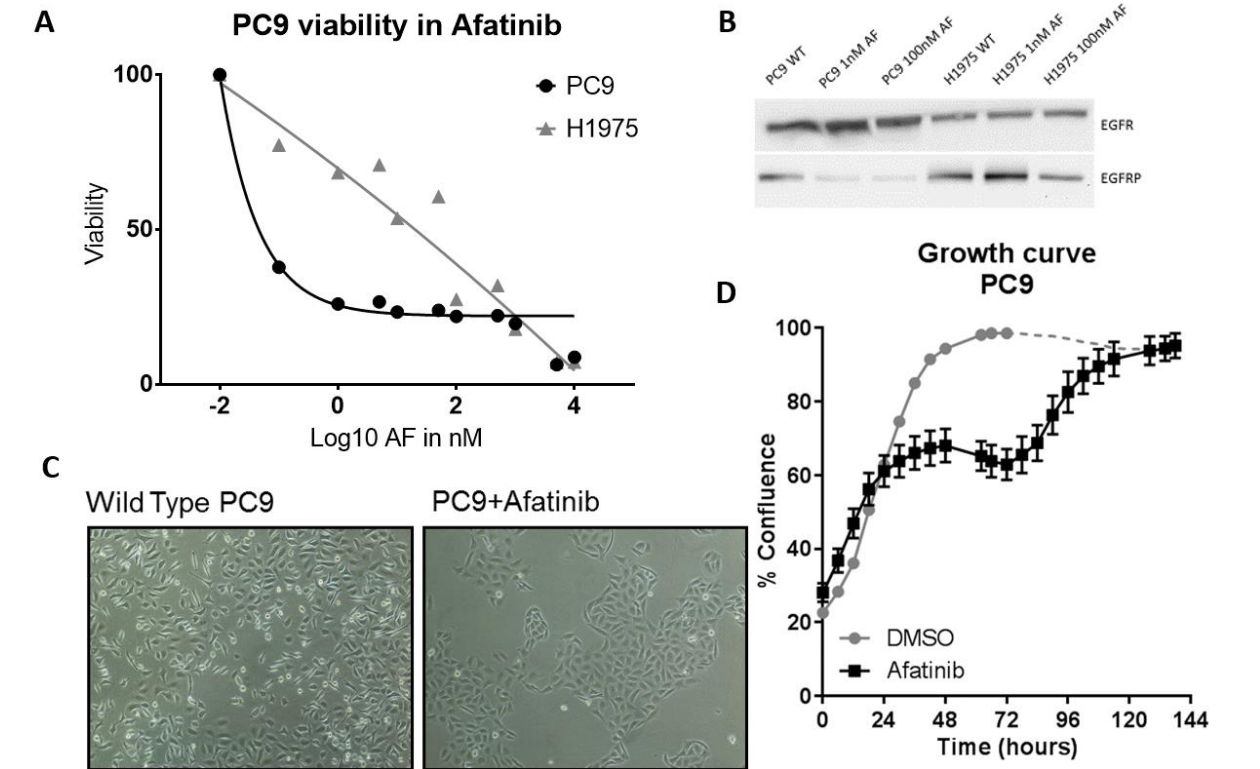


Figure 2: PC9 cells develop adaptive resistance to afatinib. **A** Viability (metabolic activity relative to wild type) of PC9 and H1975 cell lines in increasing concentrations of afatinib (log10). **B** Western Blot of PC9 and H1975 cell lines in 1 nM and 100 nM afatinib shows consistent EGFR expression and reduced EGFR Phosphorylation. **C** PC9 cells exposed to afatinib (10 nMol/L) after 24 hours are morphologically distinct from wild-type PC9. **D** PC9 cells in DMSO and 10 nMol/L afatinib medium. PC9 cell growth is inhibited in presence of afatinib. After 72 hours, the capacity for cell growth is regained and eventually reaches full confluency.

Differentially regulated protein expression and phosphorylation

After establishing the presence of adaptive afatinib resistance mechanisms in PC9 cell lines, the next challenge was to find these underlying molecular adaptations. It was unknown what proteins were responsible for the adaptive response, only that the adaptations would be at the level of protein expression and regulation. As such, a proteomic and phosphoproteomic SILAC approach allowed us to assess changes in protein regulation on a proteomic scale. PC9 cells were cultured for 1 to 7 days in 10 nM afatinib and harvested at 0 hours (T0), 24 hours (24h), 3 days (3D), 5 days (5D), and 7 days (7D) for proteomic data and T0, 20 minutes (20m), 24h, 3D and 7D for phosphoproteomic data. In addition, untreated PC9 cells were labelled with lysine-4 and arginine-6 heavy essential amino acids that would serve as an internal standard equivalent to the T0 data point. Cells were lysed and enzymatic processes inhibited. Protein digestion was done by trypsin, this ensures every resulting peptide that comes from the labelled cell line contains a heavy label. Heavy and light samples were mixed 1:1. For proteomics, samples were fractionated with high-pH chromatography, each fraction was analysed with LC-MS/MS separately.

For phosphoproteomics, samples were enriched using pY-IP before LC-MS/MS. Proteome and phosphoproteome reconstruction and quantitative analysis were done with MaxQuant. Significant differential expression was determined by Chi-squared test FDR 5% and a 2fold change (fig 3A). At 5 days the highest number of differentially expressed proteins were detected, which coincides with approaching 100% confluency and indicates the peak or just past the peak of growth in an adaptive state. Of the differentially expressed proteins, the vast majority were related to the following GO-term defined biological processes: metabolism, protein metabolism, energy pathways, and cell growth/maintenance. To a far lesser degree (<10) differentially expressed proteins were associated with: protein folding, regulation of translation, regulation of cell cycle, cytoskeleton organisation, cell adhesion, and cell migration (fig 3B).

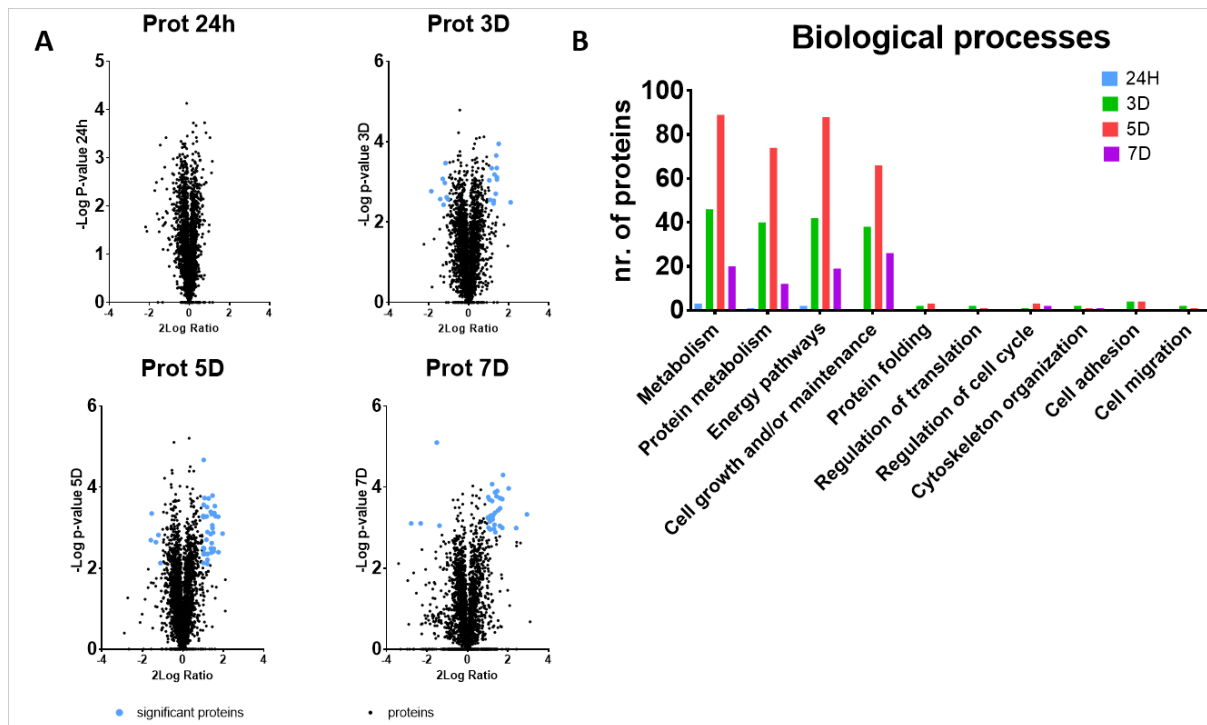


Figure 3: proteomics. **A** Volcano plot shows significant differential expression in blue. $\alpha = 0.05$, 2 fold change. **B** Proteins of significant differential expression grouped by biological process (GO terms)

In contrast to the regulation of expression, which takes hours, post-translational regulation operates on a smaller time scale of minutes. Protein phosphorylation is a prominent form of post-translational regulation of major cellular processes, such as growth. Therefore, changes in phosphorylation can tell us much about quick adaptive responses. As such, phosphoproteomic analysis can show which phosphorylation sites are up or down-regulated in this manner. After phosphotyrosine enrichment and MS analysis, differentially tyrosine-phosphorylated peptides were identified and quantified. Significant differential regulation is

determined by Chi-squared test FDR 5% and a 2 fold change. (fig. 4A). When assigned to GO terms two categories are vastly overrepresented, namely: Cell Communication and Signal transduction. A far smaller number of proteins (<5) were involved in: Regulation of cell proliferation, cell migration, wound healing, and Lipoprotein metabolism. In contrast to the proteomics data, phosphoproteomics data shows the largest change at the 7-day time point at which the cell culture has reached full confluence within the afatinib medium(fig. 4B).

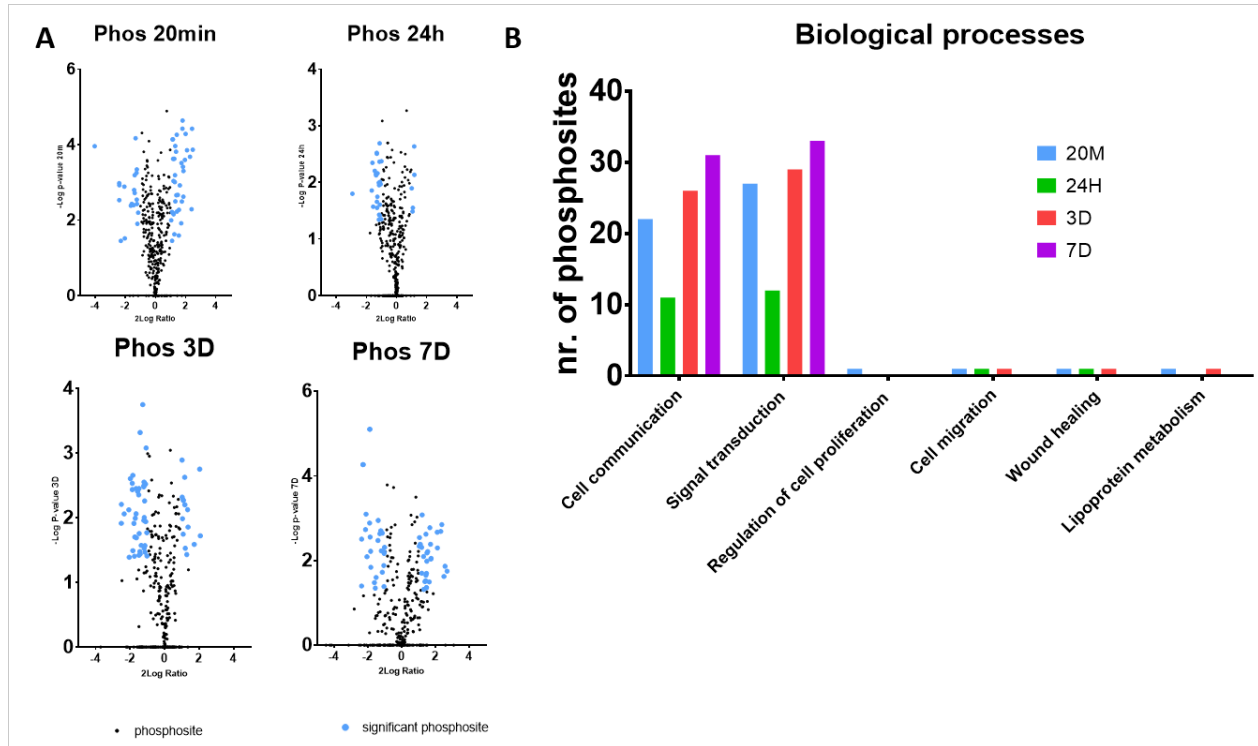


Figure 4: phosphoproteomics. **A** Volcano plot shows significant differential phosphorylation in blue. $\alpha = 0.05$. **B** Proteins of significant differential Phosphorylation grouped by biological process (GO terms).

Pattern commonalities between proteins involved in major pathways.

In exploring a pattern-based approach proteins can be associated not just through involvement in the same biological processes but also through similar behaviour. By grouping significantly differentially phosphorylated by significant change between all timepoints (ANOVA $\alpha=0.05$) or subsequent time points (T-test $\alpha = 0.05$) and the direction in which these significant changes occur, there are a number of patterns that can occur. For every change from one time-point to the next, phosphorylation levels can undergo significant upregulation, significant downregulation, and insignificant regulation. With three possibilities to 4 changes, including T0 untreated, this results in 81 patterns of up or downregulation in relation to the previous timepoint. After categorisation, phosphosites on proteins were clustered based on phosphorylation status relative to the T0. One cluster which stood out displayed a pattern of up-down-up

regulation. In this cluster, the changes were drastic and always highly upregulated and/or heavily down-regulated in comparison to wild-type phosphorylation (fig. 5). Interestingly within this cluster, phosphosites that belonged to an RTK other than EGFR, namely MET and an adaptor protein for ERBB2 (HER2): ERBB2IP (Erbin) were identified. HER2 is closely related to EGFR but is involved in microtubule organisation on the periphery of the cytosol, the differential regulator of the adaptor may suggest Erbin activity. MET plays a canonical role in neural signal transduction. While phosphorylation varied drastically over time, protein expression, as assessed by the full proteome analysis was stable, suggesting that post-translational regulation is responsible for these observed changes.

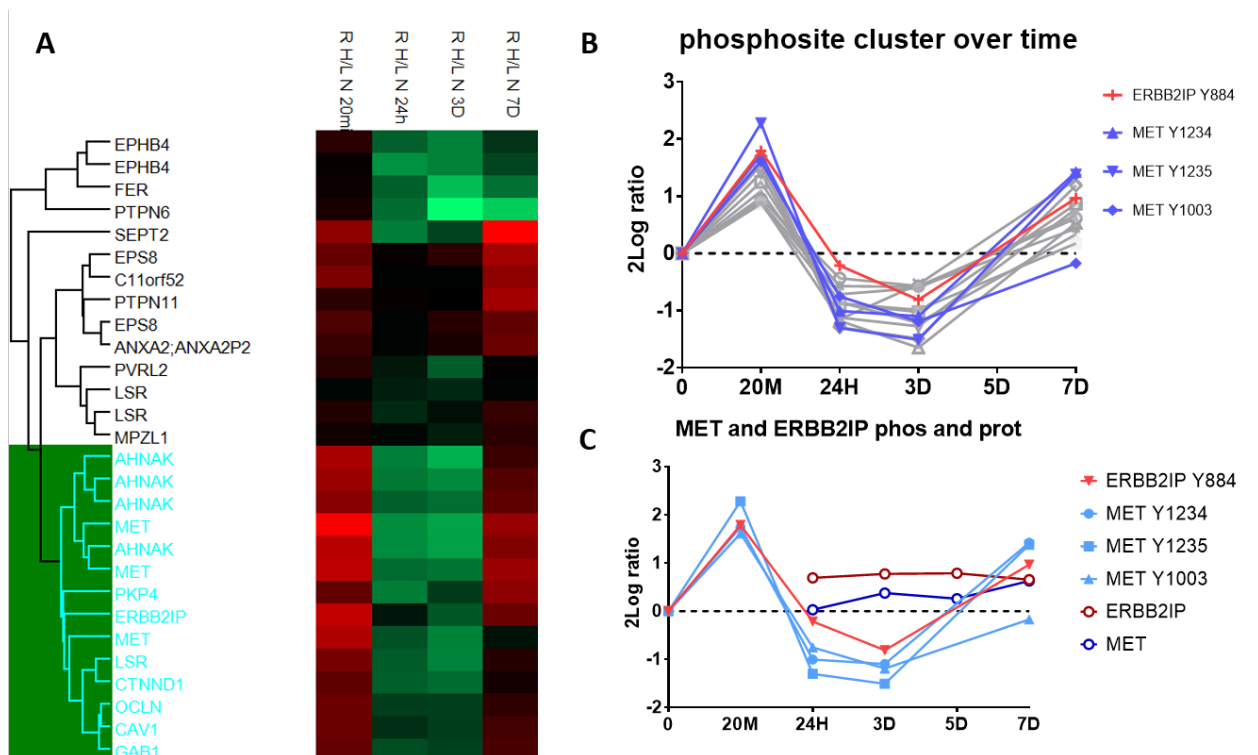


Figure 5: A A cluster within the time series shows a strong up-down-up pattern (highlighted). B Within the selected cluster in A are an RTK MET and an RTK adaptor protein for ERBB2 (HER2), ERBB2IP (Erbin) C Phosphorylation (solid) does not follow the same pattern as expression.

Another prominent Cluster showed an opposite type of pattern: down-up-down with similar drastic changes in the downregulation of phosphorylation but an apparent rescue to wild-type levels of phosphorylation on days 3 and 5 (fig. 6). This is further reinforced as this cluster happens to contain EGFR and PIK3R phosphorylation sites. Afatinib targets the cytosolic domain (669-1210). Tyrosine residues in this region are subject to cross phosphorylation, and an immediate reduction in phosphorylation of sites in this domain is to be expected. However, the return to untreated levels of phosphorylation is not to be expected. To analyse this further, combining phosphorylation data with expression data shows that the

increased phosphorylation is likely due to an increase in expression of EGFR and PIK3R over the three and five day timepoints. Despite enhanced expression, phosphorylation of EGFR Y824 and Y1152 diminishes after the 24 hour mark while PIK3R3 Y104 drops steeply after three days.

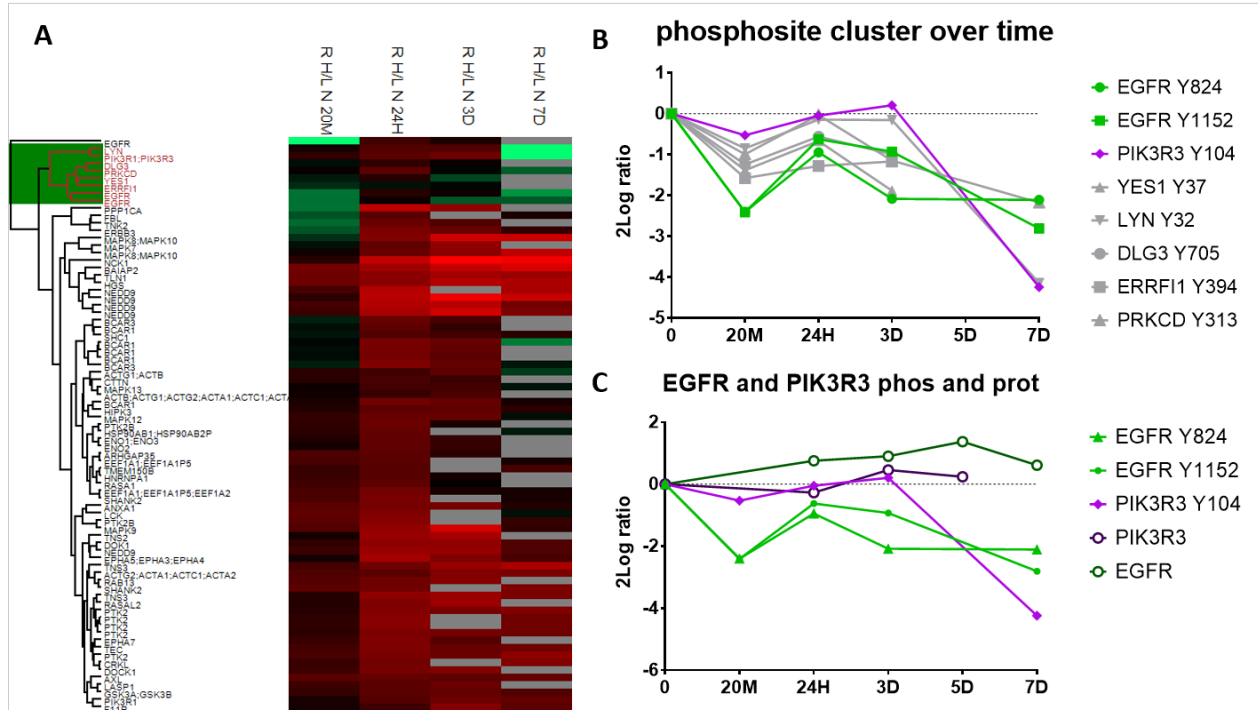


Figure 6: A A pattern of down–up–down phosphorylation is highlighted within the heatmap. B Included in this cluster are EGFR and kinase target PIK3R3. C Plotting protein expression alongside phosphorylation suggests that the increase in phosphorylation observed at 24h and 3D may be due to an increase in expression over phosphorylation.

In addition to pattern-based searching association-based searching yielded some outstanding results as well. Using Cytoscape we produced an interaction-based network of associated proteins and phosphosites, we then mapped the phosphorylation status of these residues (fig. 7). The phosphorylation state was determined by the delta of the regulation at the phosphoproteome and proteome level to correct for regulation through expression. Post-translational adaptations act on a smaller timescale than adaptations in expression. As such expression levels were assumed to resemble untreated wild-type levels at the 20 minute time point. The network features phosphorylation data of several Tyrosine Kinase receptors, notably EGFR, MET, and ERBB2. EGFR demonstrates gradual dephosphorylation over time, ERBB2IP follows much the same pattern though delayed in comparison to EGFR. ERBB2IP is an ERBB2 adaptor protein that could be a proxy for ERBB2 but may also interact with other TKRs. There is a slight increase in phosphorylation at 24 hours. MET however shows a pattern as discussed prior, where there is an initial upregulation in a short timescale, followed by a down-regulation over the 24hour and 3 day time points

and subsequent upregulation at the 7 day time point. The same pattern exists for the phosphosites included, however, Y1003 shows a greater degree of upregulation at 20 minutes and a lesser degree at 7 days than 1234 and 1235. This indicates a high degree of MET activity in the growth stage of adaptation past the 72-hour mark. Downstream signalling of EGFR: PIK3R2, JAK2, MAPK8/9/14, NCK1, PXN are affected by EGFR inhibition in unique ways which do not follow the same pattern as EGFR. PIK3R2, a subdomain of PIP3K shows a slight reduction in phosphorylation but this is returned to a level similar to the T0 level by day 7, remaining comparatively stable throughout. JAK2 phosphorylation dips at two time points, 24 hours and 7 days. Both of which coincide with periods of suspended growth. MAPK 14 is one of four p38 MAP kinases which are in a direct cascade involved in cell growth and follows a gradually increased dephosphorylation over time. MAPK 8 and 9 however show an opposing pattern of phosphorylation. Both are highly upregulated at the 24 hours and 3 day time points, MAPK8 continues this trend, however, MAPK9 is slightly down-regulated at the 7 day time point. This disparity in regulation may be due to processes involved as MAPK 8 and 9 play a role in cytoskeleton modification as do the next set of proteins. NCK1 and Paxillin(PXN) show an increasing degree of phosphorylation over time. Both proteins play an important role in cell motility, cytoskeletal organisation, and facilitating signal transduction via Tyrosine Kinase Receptor (TKR), PXN as part of an integrin-binding domain of the focal adhesion complex, and NCK1 as an adaptor protein for PXN or TKRs. ABL1 is a protein associated with cytoskeletal modulation as well but is involved in more processes related to cell survival. Despite this, it is dephosphorylated at the 20 minute and 7 days timepoints and shows similar phosphorylation to wild-type untreated cells at 24 hours and 3 days. ABL1 regulating ABI1 shows a similar pattern. Finally, CAV1 is a Calcium Ion channel that is involved in cell adhesion and E-cadherin and B-catenin availability under influence of EGFR. Phosphorylation state differs greatly per phosphosite, Y6 becomes dephosphorylated, Y14 shows a pattern much like MET; up at 20 min, down at 24 hours, down at 3 days, and upregulated at 7 days, Y25 shows only slight dephosphorylation over time.

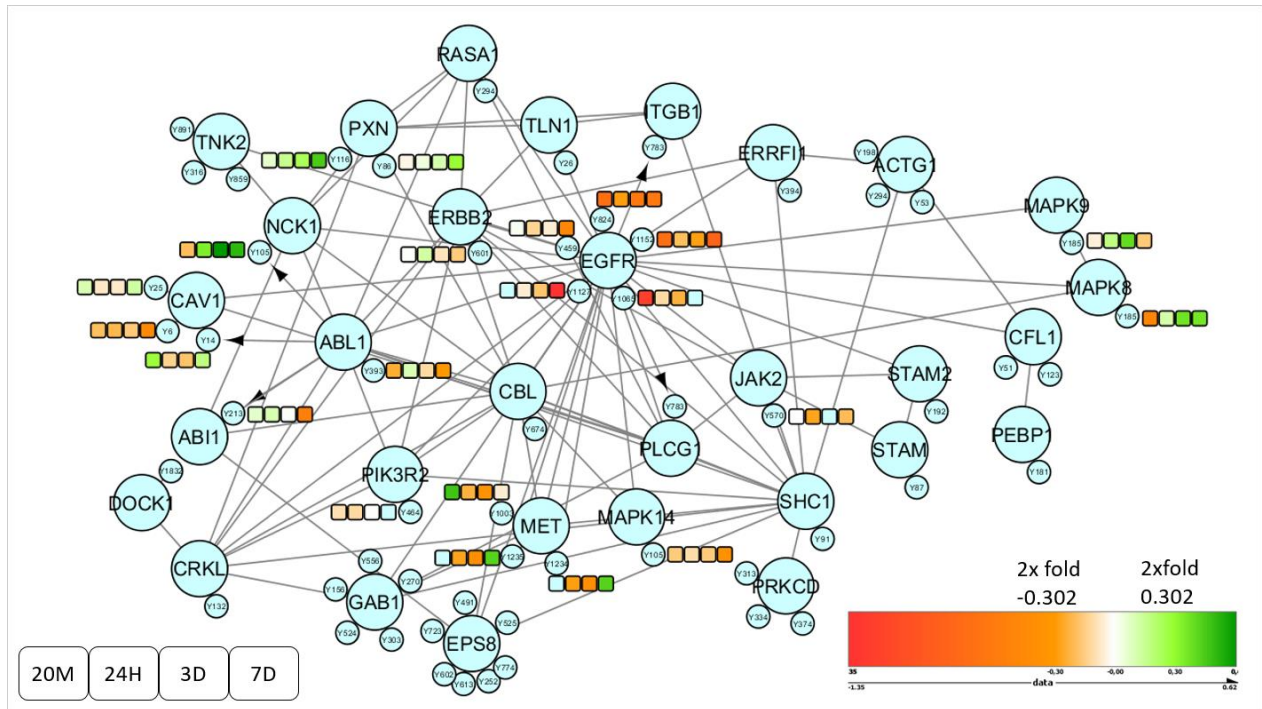


Figure 7: Cytoscape protein network shows protein interactions as strings. The large circles are proteins, the smaller circles are phosphorylation sites, the series of four boxes represent the phosphorylation of that phosphosite over time. The colour gradient shows the level of phosphorylation for each site compared to the wild-type phosphorylation and is corrected for expression levels.

Discussion

PC9 adaptive afatinib resistance depends on cell-cell proximity

PC9 and H1975 cells were treated with 1 – 100 nM afatinib and subsequently assessed using almar blue viability assay. PC9 cells show viability of ~20% of untreated PC9 cells (fig. 2A, B). This could be ascribed to a subpopulation of PC9 cells intrinsically resistant to afatinib. However, ~20% viability was consistent across repeated assays and PC9 cells were cultured a limited amount of turns to prevent Heterogeneity. In a homogenous population of PC9 cells sensitive to afatinib, the occurrence of afatinib resistance in a subset of the population cannot be genetic in origin. There could be a physiological condition to which this consistent fraction of cells adhere to. In this study, cell cycles were not synchronised. It is possible that cell cycle stage predisposes cells for survival. Yong-an Song *et al.* 2019 demonstrated that apatinib (VEGFR inhibitor) treatment of PC9GP cells (PC9 derivative) arrests cell growth at the first growth(G1) phase of the cell cycle²⁹. This situation seems phenotypically similar to afatinib treatment of PC9 cells. Afatinib could be less effective at initiating apoptosis in G1 cells, selecting for cells residing in the G1 stage at the onset of treatment. However, cell cycle phase G1 is also a quiescent stage where cell growth can be safely halted indefinitely in response to external factors such as the presence of afatinib.

Continued afatinib exposure inhibited cell growth and intercellular organisation (fig. 2C, D). 24 hours after afatinib introduction growth had stopped and the remaining cells had clustered together into secluded islets. At 72 hours, cell growth had initiated again until complete confluence at 7 days. Cell clustering is not a prerequisite for growth arrest, as such if the cell cycle phase is the cause for survival, cell clustering is a response. No cell motility assay was performed in this study. However, Mulder *et al.* 2018 showed in a scratch assay that after 24 hours of 10nM afatinib treatment PC9 motility is reduced drastically compared to wild type³⁰. This evidence suggests that cells do barely move once afatinib treatment is initiated. The Islet phenotype observed after 24 hours of afatinib treatment indicates areas of high cell density exist prior to event onset and may have a direct causal link to survival. In absence of pre-existing subpopulations of genetically resistant PC9 cells, only regulation at a post-transcriptional level remains as an attractive explanation for the observed phenotype. Two phenotypic adaptations 24 hours after treatment onset were observed; cell growth stopped and cells clustered together in dispersed islets. Owing to the lack of cell motility upon afatinib exposure, the topographically agnostic G1 selection hypothesis is unlikely as this alone would not result in the Islet phenotype without cell migration. The inverse is more likely, where cells within high-density patches have a higher chance of survival due to proximity to other cells and enter a quiescent G1 stage as EGFR is inhibited. There may be a combined effect where residing in the G1 phase before treatment modulates the chance of survival for cells in high-density positions or more cells in high-density positions are in G1 at a given time, but we cannot confirm either.

MET, Paxillin, and NCK1 upregulation may rescue downstream EGFR signal transduction independent of EGFR through Integrin-RTK cross-talk.

Proteomic and phosphoproteomic analysis allowed us to observe adaptive changes to protein expression and tyrosine phosphorylation as NSCLC cells survive and subsequently grow in 10 nM afatinib. Of the differentially expressed proteins, the main categories are all directly linked to such a process. (Protein) Metabolism changes depending on need. Cell signaling and cell growth regulation are linked and afatinib specifically inhibits the latter through EGFR inhibition. Significant differences in post-translational regulation of phosphorylation were seen in signal transduction again but more importantly in cell communication specifically. This would indicate that there is an important phosphorylation component in re-routing signal transduction pathways to maintain homeostasis. Interestingly the number of proteins differentially expressed peaks at 5 days while phosphorylation peaks at 7. Day 5 is around where the growth curve is at its steepest, indicating the greatest amount of growth-related activity, while at day 7 the cells approach 100% confluence and slow down growth or stop in many cases (fig. 2D). What this

illustrates is that changes in expression levels may, in general, be more related to facilitating proliferation and phosphorylation plays a larger role in maintaining baseline signals required for continued survival. Nevertheless, both modes of adaptation play a role to an extent in survival and growth. MET is an RTK that shows a significant upregulation in phosphorylation after 20 minutes already at Y1003, Y1234, Y1235. All three of these residues are associated with MET activation³¹. ERBB2IP-Y884 follows the same patterns as MET-Y1003, MET-Y1234, and MET 1235 but is not associated with any known Erbin activity³¹. While ERBB2IP-Y884 phosphorylation is upregulated at 20 min, no upregulation of ERBB2 (HER2) phosphosites was detected at this timepoint including ERBB2-Y601 which is not associated with any known ERBB2 regulation³¹ (fig. 7). The similarity in phosphorylation pattern between Erbin and MET could suggest novel interaction between Erbin and MET or ERBB2 activation similar to MET as a result of afatinib treatment. This response however is cut short as at 24 hours and 3 days after treatment this duo is heavily downregulated. In contrast, EGFR expression seems to compensate for reduced phosphorylation of EGFR on multiple tyrosine residues; Y824 (Y827), Y1152, Y1065 (Y1069), Y459, Y1127 (Y1125). This suggests that there is a high threshold for EGFR inhibition required before MET-mediated rescue becomes a viable alternative. However, when at day 7 MET phosphorylation is elevated once again, high levels of EGFR expression are not enough to keep a functional level of EGFR activity. This further reinforces a compensatory role for MET once EGFR activity falters. First within the timeframe expression level compensation cannot occur, after 20 minutes of treatment, and a second time when an increased expression is no longer enough at 7 days. To add to the importance of RTK signaling in response to afatinib, ABL interacting protein (ABI1) activity is heavily regulated at Y213 throughout the adaptation process. ABI regulates endocytosis of EGFR and other RTKs and therefore plays a role in the retention of RTKs at the cell surface³². At 20 min and 24 hours, we observed a slight increase in phosphorylation, base-level phosphorylation at 3 days, and downregulation of phosphorylation at 7 days. The increased phosphorylation of MET at 20 min, subsequent reduction in phosphorylation of MET, and the increased EGFR expression at 24 hours before adopting elevated MET phosphorylation, may go some way to explaining the early upregulation in response to a rapid turn-over in RTK reliance. While down-regulation at later time points could mark an increase in retention of alternative RTKs, like MET, as EGFR expression fails to compensate for inhibition. In addition to MET up-, down- and subsequent upregulation, some Cytoskeleton, and RTK related proteins are phosphorylated to a higher degree after 24h of afatinib exposure. Cytoskeleton organising MAP Kinases MAP8 and MAP9 are both continuously upregulated at activating phosphosite Y185 after 24h, with exception of MAP9 at day 7. Focal adhesion – Actin connective protein Paxillin is phosphorylated on Y86

(Y88) and Y116 (Y118), the latter corresponds with general activity and the former is associated with erlotinib treatment³¹. Actin-associated RTK adaptor NCK1 is phosphorylated at Y104 (Y105), another site associated with erlotinib³¹. Both paxillin and NCK1 phosphosites show a regulatory pattern similar to MAP8 (fig 7). The association of NCK1-Y104 and PXN-Y86 with erlotinib treatment as well as Paxillin phosphorylation being linked to cisplatin resistance suggests a specific adaptive role for both³³. Paxillin and NCK1 are involved in cross-talk between RTKs and another family of transmembrane signaling proteins; Integrins³⁴⁻³⁶. While we lack information on Integrin expression, the increase in phosphorylation of these related proteins may indirectly support an adaptive role for integrin-based signaling^{34,37-39}. Integrins in and of themselves form an important receptor for cell survival but can also cross talk with mainly EGFR, but also MET⁴⁰. In doing so they can activate PI3K and RAP pathways as well as concentrating and retaining RTK at the cell membrane, Amplifying RTK signaling³⁴. The increase of EGFR expression observed on days 3 and 5 may partially be due to this retention. Within this integrin-RTK cross-talk complex, MET may take over from EGFR after day 5, due to the observed phosphorylation levels at day 7 for both RTKs. Finally, Integrin also plays a role in cyclin kinase regulation, this cell cycle control could contribute to the G1 locking suggested earlier^{29,41}. JAK2 is a part of the JAK/STAT pathway which operates downstream of EGFR. Signal transduction is regulated through JAK2JH2 which phosphorylates JAK2-Y570 specifically and in doing so inhibits JAK2 signaling⁴². We observe continuous depletion of JAK2-Y570, this may suggest a necessity of greater JAK2 availability despite EGFR inhibition, indicating JAK/STAT signaling is retained during adaptation. In the same vein, while there is a PIK3R3 phosphopeptide which is remarkably similar in down-regulation to EGFR (fig. 6), PIK3R3-Y104 does not correspond with a known regulatory function. PIK3R2-Y465 (Y464) however, is a phosphosite that is associated with PI3K activity through the PIK3R2 subunit and has phosphorylation levels similar to T0. PI3K is an essential signal for cell survival and growth which operates directly downstream of EGFR. The retention of PI3K signaling while EGFR is inhibited suggests an adaptive response upstream of PI3K. An attractive candidate for such an adaptive alternative is the Integrin-RTK cross-talk suggested prior. Yoshida *et al.* 2014 observed a similar regulatory adaptation in conjunction with EGFR T790M mutation, induced in PC9 cells. Stating an alteration upstream of PI3K and an 11fold increase in MET activity without gene duplication⁴³.

Caveolin-1 may help intercellular adhesion and enhance PI3K signaling through TIE2-angiopoietin connections

Caveolin-1 (Cav1) is a calcium ion channel that is associated with oligomeric lipid rafts which become caveolae through Cavin activity and eventually clathrin-independent endocytosis. Furthermore, Cav1

inactivity is associated with loss of polarity characteristic of epithelial tissues and is therefore linked with metastatic potency⁴⁴⁻⁴⁶. Of the Cav1 phosphosites, Y14 is associated with Cav1 activation and Y25 phosphorylation is associated with Su11274 treatment³¹. Both these phosphosites showed a regulation pattern, high-low-low-high, which was reminiscent of MET and Erbin (fig. 5). Although the specific function of Y25 phosphorylation is unknown, the link to Su11274 is potentially significant as Su11274 is a MET inhibitor and co-treatment with afatinib appears to have a synergistic effect on T790M NSCLC cells^{47,48}. The third phosphosite, Y6, is continuously down-regulated and associated with EGF treatment. The specific function of Y6 phosphorylation is also unknown but may relate to invagination of caveolae and endocytosis if the following hypothesis is plausible. Cav1 is able to recruit TIE2 directly to caveolae and is phosphorylated at Y14 by TIE2, this RTK promotes angiogenesis and overlaps with EGFR in PI3K pathway activation among other survival signals. Furthermore, TIE2 has membrane-bound ligands, angiopoietin, which can help reinforce cell-cell interactions in a way similar to integrins. Although we lack specific information on TIE2 expression, ABI downregulation may also help TIE2-Cav1 containing lipid rafts to be retained at the cell surface. Finally, the similarity between Cav1-Y14 and Cav1-Y25 and MET phosphorylation in addition to Cav1-Y25 association with Su11274 suggests a strong link between Cav1, MET, and possibly TIE2 which is deserving of further investigation.

Conclusion

The ability of PC9 cells to survive treatment with 10 nM afatinib is heavily reliant on cell-cell adhesion. Both morphological and proteomic data point towards a greater importance of juxtacrine interactions following EGFR inhibition. In addition, cells adapt to using different and seemingly less favorable RTKs for growth and survival, such as MET. MET may be up-regulated within the first 20 minutes to mitigate cell death, then down-regulated as EGFR expression is increased after less than 24 hours and allows restoration of EGFR signaling until after 3 days this restoration appears to be insufficient and MET signaling is once again required. This study opens several avenues of inquiry; The possibility of Erbin interactions with other RTKs than HER2. Which RTKs and the extent to which they can rescue EGFR signaling. The importance of Integrin cross-talk in adaptive resistance and how inhibition affects cell viability. The specific functions of several phosphosites; PIK3R3-Y104, NCK1-Y104, PNX-Y86, and Cav1-Y25. Finally, the potential role of Cav1, MET, and TIE2 in an adaptive mechanism parallel to integrin cross-talk.

Materials and Methods

Cell

Culture

Cell culture NCI-H1975 was acquired from the ATCC, PC9 was derived from Sigma. EGTA and Lanthanum (III) Chloride Hydrate were purchased from Sigma Aldrich. afatinib was purchased from Selleckchem. RPMI medium, Pen/Strep, and L-glutamine were purchased from Lonza, FBS from Thermo and light amino acid depleted DMEM from Buchem BV.

Cells were incubated at 37° C at 5% CO₂ in RPMI medium with 1% Pen/Strep, 10% FBS and L-glutamine. Cells were controlled for mycoplasma infection and were kept for no more than 7 plating cycles. Cells cultured for proteomics were treated the same way but RPMI medium was replaced with light amino acid depleted DMEM containing Arginine-6 and lysine-4 for SILAC labelling. These cell cultures underwent at least 5 plating cycles to ensure complete labelling. Afatinib was administered through liquid medium renewal 24 hours after plating. Harvesting for proteomics occurred at afatinib treatment (T0), 24 hours after treatment (24h), three days after treatment (3D, 72h), five days after treatment (5D,120h), and seven days after treatment (7D, 144h). For phosphoproteomics, harvesting moments were at afatinib treatment (T0), 20 minutes after treatment (20 min), 24 hours after treatment (24h), three days after treatment (3D), and 7 days after treatment (7D). Cell processes were stopped by placing plates on ice.

Viability,

Growth

An InuCyte System was acquired from Essen Bioscience. AlmarBlue Cell Viability Assay was purchased from Thermo Fisher Scientific. Growth was measured using the InuCyte System with 1,500 cells per 69-well plate. Cell viability was assessed through AlmarBlue Cell Viability Assay and curves fit with non-linear fit curve fitting in GraphPad Prism 7. Cells were treated 72 hours prior to analysis with an increasing afatinib concentration ranging from 0.01- 1,000 nM.

Cell

lysis

Protease (Complete mini tablet, EDTA-free) and phosphatase inhibitors (PhosSTOP tablet) were purchased from Roche, Chloroacetamide, trypsin at Sigma, and PBS from Lonza. Desalting column sep-pak C18 (1cc: 50 mg) was obtained from Waters Corp.

Following Cell culture, cells were washed with PBS then lysed. For proteomics, lysis took place in 1% SDC, 10 mM TCEP, 100 mM TRIS, 40 mM Chloroacetamide, Protease inhibitors, and Phosphatase inhibitors. Next, these were mechanically aided through sonification for 15 cycles, 30 seconds each at a 30-second interval. For Phosphoproteomics, cells were lysed in 7 M urea, 1% triton, 100 mM TRIS, 5 mM TCEP, 30 mM CAA, 10 units/mL DNase1, 1mM pervanadate, 1% Benzonase, 2.5 mM Mg²⁺, Phosphatase

inhibitor, and protease inhibitor. Next proteins were precipitated with methanol/chloroform and digested overnight with Trypsin. Finally, remaining peptides were desalted with the Seppack C18 column.

Western blotting

Precast gel (12% SDS) and Transfer buffer 1x TG, 20% ethanol were purchased from Bio-rad. Secondary antibodies from Dako and Pierce ECL Plus Substrate from Thermo. Primary antibodies EGFR-pTyr1068 and Actin came from Abcam. EGFR antibodies were from Cell Signalling Technology.

20 – 30 µg cell lysate was run on the precast gel then transferred to PVDF membrane in transfer buffer and blocked with 5% milk or BSA. Primary antibody incubation was done overnight at 4° C, secondary antibodies for 2 hours at 20° C before visualisation using Pierce ECL Plus Substrate.

HPLC, Ptyr-IP and Mass Spectrometry

Proteomics peptide samples were fractionated by hydrophobicity using high pH liquid chromatography on an Agilent 1200 HPLC system. 100 µg cell lysate was loaded in a buffer A of 10 mM NH₄OH (pH 10) and eluted using a gradient of buffer B consisting of 10 mM NH₄OH in 90% ACN (pH 10). Fractions produced were loaded separately onto the mass spectrometer.

For phosphoproteomics, Phosphotyrosine peptide enrichment was done with Phosphotyrosine immunoprecipitation (pY-IP). After proteolytic digestion, samples were loaded onto the anti-pY containing agarose beads, supernatant removed, beads washed, and enriched phosphopeptides eluted. (pY-IP protocol and source could not be retrieved) Samples were stored at -80° C before loading onto the mass spectrometer.

Proteomic and phosphoproteomic analysis took place on a liquid chromatography tandem mass spectrometer (LC-MS/MS); Agilent 1290 LC from Agilent Technologies coupled to an Orbitrap Q-Exactive HF from Thermo. Liquid Chromatography

Data analysis

RAW files were processed using MaxQuant. Once qualitative and quantitative data was assigned to proteins further analysis was done using Perseus (v. 1.5.0.0). Patterns of Differential expression and regulation were determined through t-test between time points (FDR 5%) and positive or negative delta from one time point to the next. ANOVA was also performed on all time points together (FDR 5%). Protein network was produced using Cytoscape (3.4.0), Phosphosite regulation was determined as the difference between phosphopeptide and protein expression level as measured through MS. Some phosphosites did not line up with reference data from PhosphositePlus³¹. In cases where there was no Tyrosine residue in at this location, we assigned Tyr phosphosite within ~5 residues if there were no others nearby. We

assumed this was an artefact on our end. Phosphosites treated in this way were; (Data → Reference)
EGFR-Y824 → Y827, EGFR-Y1065 → Y1069, EGFR-Y1127 → Y1125, PXN-Y86 → Y88, PXN-Y116 → Y118,
NCK1-Y104 → Y105, PIK3R3-Y465 → Y464.

References

1. Vogelstein, B. *et al.* Cancer genome landscapes. *Science* vol. 340 1546–1558 (2013).
2. Lenz, L. S. *et al.* Cancer cell fitness is dynamic. *Cancer Res.* **81**, 1040–1051 (2021).
3. Rozhok, A. I. & DeGregori, J. The three dimensions of somatic evolution: Integrating the role of genetic damage, life-history traits, and aging in carcinogenesis. *Evol. Appl.* **13**, 1569–1580 (2020).
4. Wei, J. *et al.* Clinical Value of EGFR Copy Number Gain Determined by Amplicon-Based Targeted Next Generation Sequencing in Patients with EGFR-Mutated NSCLC. *Target. Oncol.* **16**, 215–226 (2021).
5. Hirsch, F. R. *et al.* Epidermal growth factor receptor in non-small-cell lung carcinomas: Correlation between gene copy number and protein expression and impact on prognosis. *J. Clin. Oncol.* **21**, 3798–3807 (2003).
6. Levine, A. J. Reviewing the future of the P53 field. *Cell Death Differ.* **25**, 1–2 (2018).
7. Rusch, V. *et al.* Differential Expression of the Epidermal Growth Factor Receptor and Its Ligands in Primary Non-Small Cell Lung Cancers and Adjacent Benign Lung. *Cancer Res.* **53**, 2379–2385 (1993).
8. Brodsky, F. M. Monoclonal Antibodies as Magic Bullets. *Pharm. Res. An Off. J. Am. Assoc. Pharm. Sci.* **5**, 1–9 (1988).
9. Lee, Y. T., Tan, Y. J. & Oon, C. E. Molecular targeted therapy: Treating cancer with specificity. *Eur. J. Pharmacol.* **834**, 188–196 (2018).
10. Xie, Y. H., Chen, Y. X. & Fang, J. Y. Comprehensive review of targeted therapy for colorectal cancer. *Signal Transduct. Target. Ther.* **5**, (2020).
11. Oh, D. Y. & Bang, Y. J. HER2-targeted therapies — a role beyond breast cancer. *Nat. Rev. Clin. Oncol.* **17**, 33–48 (2020).
12. Barr Kumarakulasinghe, N., Zanwijk, N. Van & Soo, R. A. Molecular targeted therapy in the treatment of advanced stage non-small cell lung cancer (NSCLC). *Respirology* **20**, 370–378 (2015).
13. Lin, N. U. *et al.* A phase II study of afatinib (BIBW 2992), an irreversible ErbB family blocker, in patients with HER2-positive metastatic breast cancer progressing after trastuzumab. *Breast Cancer Res. Treat.* **133**, 1057–1065 (2012).
14. Kobayashi, S. *et al.* *Harvard Medical School; the Departments of Cancer Bi-ology. Deaconess Medical Center* www.nejm.org (2005).
15. Wu, S. G. *et al.* The mechanism of acquired resistance to irreversible EGFR tyrosine kinase inhibitor-afatinib in lung adenocarcinoma patients. *Oncotarget* vol. 7 www.impactjournals.com/oncotarget/ (2016).
16. Hashida, S. *et al.* Acquisition of cancer stem cell-like properties in non-small cell lung cancer with

- acquired resistance to afatinib. *Cancer Sci.* **106**, 1377–1384 (2015).
17. Ferguson, F. M. & Gray, N. S. Kinase inhibitors: The road ahead. *Nat. Rev. Drug Discov.* **17**, 353–376 (2018).
 18. Oddo, D. *et al.* Molecular landscape of acquired resistance to targeted therapy combinations in BRAF-mutant colorectal cancer. *Cancer Res.* **76**, 4504–4515 (2016).
 19. Haas, L. *et al.* Acquired resistance to anti-MAPK targeted therapy confers an immune-evasive tumor microenvironment and cross-resistance to immunotherapy in melanoma. *Nat. Cancer* **2**, 693–708 (2021).
 20. Burrell, R. A. & Swanton, C. Tumour heterogeneity and the evolution of polyclonal drug resistance. *Mol. Oncol.* **8**, 1095–1111 (2014).
 21. Burrell, R. A., McGranahan, N., Bartek, J. & Swanton, C. The causes and consequences of genetic heterogeneity in cancer evolution. *Nature* **501**, 338–345 (2013).
 22. Sharma, S. V. *et al.* A Chromatin-Mediated Reversible Drug-Tolerant State in Cancer Cell Subpopulations. *Cell* **141**, 69–80 (2010).
 23. Vailati-Riboni, M., Palombo, V. & Loor, J. J. What are omics sciences? *Periparturient Dis. Dairy Cows A Syst. Biol. Approach* 1–7 (2017) doi:10.1007/978-3-319-43033-1_1.
 24. Ruprecht, B. *et al.* Evaluation of Kinase Activity Profiling Using Chemical Proteomics. *ACS Chem. Biol.* **10**, 2743–2752 (2015).
 25. Hu, Q. *et al.* The Orbitrap: A new mass spectrometer. *J. Mass Spectrom.* **40**, 430–443 (2005).
 26. Eliuk, S. & Makarov, A. Evolution of Orbitrap Mass Spectrometry Instrumentation. *Annu. Rev. Anal. Chem.* **8**, 61–80 (2015).
 27. Mann, M. Functional and quantitative proteomics using SILAC. *Nat. Rev. Mol. Cell Biol.* **7**, 952–958 (2006).
 28. Steen, H., Kuster, B., Fernandez, M., Pandey, A. & Mann, M. Tyrosine phosphorylation mapping of the epidermal growth factor receptor signaling pathway. *J. Biol. Chem.* **277**, 1031–1039 (2002).
 29. Song, Y. A. *et al.* Apatinib preferentially inhibits PC9 gefitinib-resistant cancer cells by inducing cell cycle arrest and inhibiting VEGFR signaling pathway. *Cancer Cell Int.* **19**, 1–15 (2019).
 30. Mulder, C. *et al.* Adaptive resistance to EGFR-targeted therapy by calcium signaling in NSCLC cells. *Mol. Cancer Res.* **16**, 1773–1784 (2018).
 31. Hornbeck, P. V. *et al.* PhosphoSitePlus, 2014: Mutations, PTMs and recalibrations. *Nucleic Acids Res.* **43**, D512–D520 (2015).
 32. Tanos, B. E. & Pendergast, A. M. Abi-1 forms an epidermal growth factor-inducible complex with Cbl: Role in receptor endocytosis. *Cell. Signal.* **19**, 1602–1609 (2007).
 33. Wu, D. W. *et al.* Phosphorylation of paxillin confers cisplatin resistance in non-small cell lung cancer via activating ERK-mediated Bcl-2 expression. *Oncogene* **33**, 4385–4395 (2014).
 34. Alam, N. *et al.* The integrin - Growth factor receptor duet. *J. Cell. Physiol.* **213**, 649–653 (2007).
 35. Zhong, X. & Rescorla, F. J. Cell surface adhesion molecules and adhesion-initiated signaling:

- Understanding of anoikis resistance mechanisms and therapeutic opportunities. *Cell. Signal.* **24**, 393–401 (2012).
36. Wang, H. Y. *et al.* Non-small-cell lung cancer cells combat epidermal growth factor receptor tyrosine kinase inhibition through immediate adhesion-related responses. *Onco. Targets. Ther.* **9**, 2961–2973 (2016).
 37. Wang, C. *et al.* Acquired resistance to EGFR TKIs mediated by TGF β 1/integrin B3 signaling in EGFR-mutant lung cancer. *Mol. Cancer Ther.* **18**, 2357–2367 (2019).
 38. Fu, Y. *et al.* Abnormally activated OPN/integrin α V β 3/FAK signalling is responsible for EGFR-TKI resistance in EGFR mutant non-small-cell lung cancer. *J. Hematol. Oncol.* **13**, 1–15 (2020).
 39. Morello, V. *et al.* B1 integrin controls EGFR signaling and tumorigenic properties of lung cancer cells. *Oncogene* **30**, 4087–4096 (2011).
 40. Ju, L. & Zhou, C. Association of integrin beta1 and c-MET in mediating EGFR TKI gefitinib resistance in non-small cell lung cancer. *Cancer Cell Int.* **13**, 1–8 (2013).
 41. Schwartz, M. A. & Assoian, R. K. Integrins and cell proliferation: Regulation of cyclin-dependent kinases via cytoplasmic signaling pathways. *J. Cell Sci.* **114**, 2553–2560 (2001).
 42. Ungureanu, D. *et al.* The pseudokinase domain of JAK2 is a dual-specificity protein kinase that negatively regulates cytokine signaling. *Nat. Struct. Mol. Biol.* **18**, 971–976 (2011).
 43. Yoshida, T. *et al.* Tyrosine phosphoproteomics identifies both codrivers and cotargeting strategies for T790M-related EGFR-TKI resistance in non-small cell lung cancer. *Clin. Cancer Res.* **20**, 4059–4074 (2014).
 44. Huang, T., Zhou, F., Wang-Johanning, F., Nan, K. & Wei, Y. Depression accelerates the development of gastric cancer through reactive oxygen species-activated ABL1 (Review). *Oncol. Rep.* **36**, 2435–2443 (2016).
 45. Burgy, M. *et al.* Cav1/ereg/yap axis in the treatment resistance of cav1-expressing head and neck squamous cell carcinoma. *Cancers (Basel)*. **13**, 3038 (2021).
 46. Lu, Z., Ghosh, S., Wang, Z. & Hunter, T. Downregulation of caveolin-1 function by EGF leads to the loss of E-cadherin, increased transcriptional activity of β -catenin, and enhanced tumor cell invasion. *Cancer Cell* **4**, 499–515 (2003).
 47. Ma, P. C. *et al.* Functional expression and mutations of c-Met and its therapeutic inhibition with SU11274 and small interfering RNA in non-small cell lung cancer. *Cancer Res.* **65**, 1479–1488 (2005).
 48. Chen, G. *et al.* Synergistic Effect of Afatinib with Su11274 in Non-Small Cell Lung Cancer Cells Resistant to Gefitinib or Erlotinib. *PLoS One* **8**, e59708 (2013).

Supplements

Supplementary Table 1: Overview of phosphosites discussed in this paper.

Protein	Phosphosite	PhosphositePlus	PhosphositePlus function (Up-/Downstream)
ABI1	Y213	Y213	Molecular association & altered endocytosis
Cav1	Y6	Y6	no known function
Cav1	Y14	Y14	Cav1 activation
Cav1	Y25	Y25	associated with Su11274
EGFR	Y459	n/a	no known function
EGFR	Y824	Y827	EGFR activation
EGFR	Y1065	Y1069	EGFR activation
EGFR	Y1127	Y1125	EGFR activation
EGFR	Y1152	n/a	no known function
ERBB2	Y601	n/a	no known function
JAK2	Y570	Y570	JAK2JH2 mediated JAK2 inhibition
MAP8	Y185	Y185	MAP8 activation
MAP9	Y185	Y185	MAP9 activation
MET	Y1235	Y1235	MET activation
MET	Y1003	Y1003	MET activation
NCK1	Y104	Y105	Associated with erlotinib
PIK3R2	Y465	Y464	PI3K activation
PIK3R3	Y104	n/a	no known function
PXN	Y86	Y88	Associated with erlotinib
PXN	Y116	Y118	PXN activation